**Cell Reports, Volume *35***

## Supplemental information

# Antiviral drug screen identifies DNA-damage response inhibitor as potent blocker of SARS-CoV-2 replication

**Gustavo Garcia Jr., Arun Sharma, Arunachalam Ramaiah, Chandani Sen, Arunima Purkayastha, Donald B. Kohn, Mark S. Parcells, Sebastian Beck, Heeyoung Kim, Malina A. Bakowski, Melanie G. Kirkpatrick, Laura Riva, Karen C. Wolff, Brandon Han, Constance Yuen, David Ulmert, Prabhat K. Purbey, Phillip Scumpia, Nathan Beutler, Thomas F. Rogers, Arnab K. Chatterjee, Gülsah Gabriel, Ralf Bartenschlager, Brigitte Gomperts, Clive N. Svendsen, Ulrich A.K. Betz, Robert D. Damoiseaux, and Vaithilingaraja Arumugaswami**

**SUPPLEMENTARY FIGURES**

Figure S1

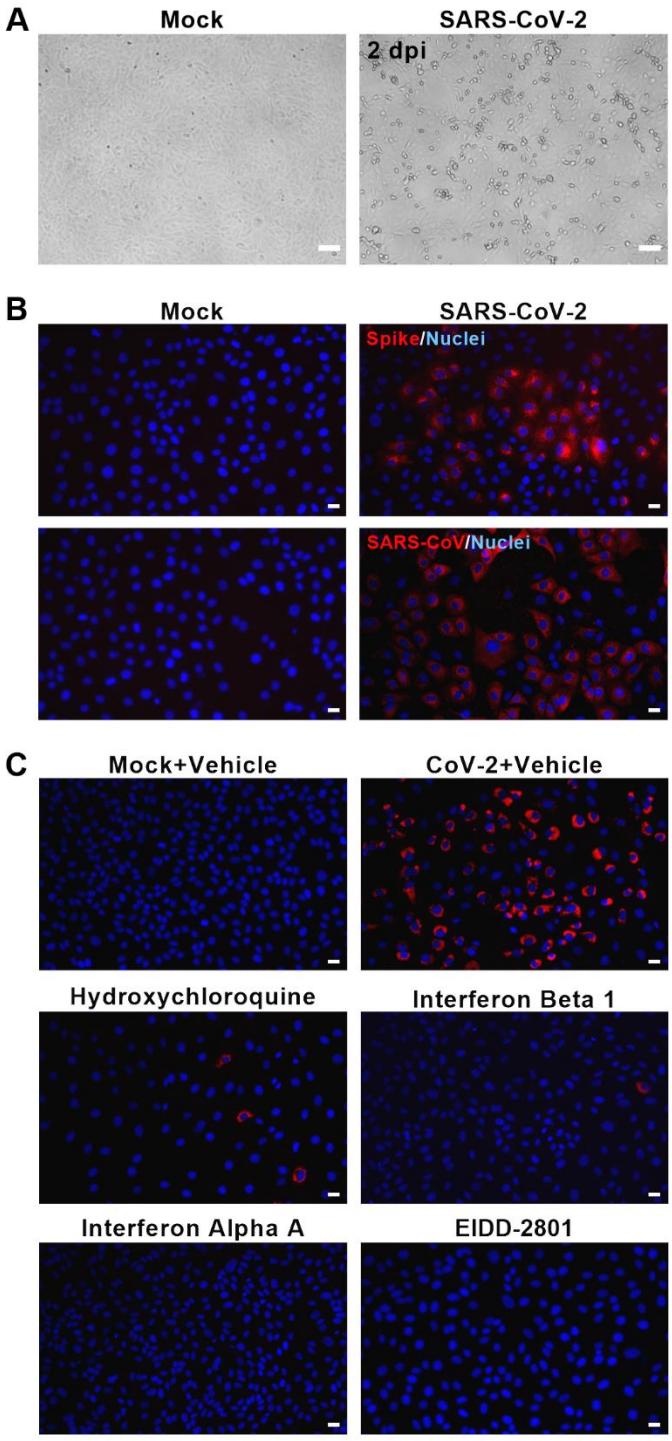

**Figure S1. Infectious SARS-CoV-2 cell culture system.** (A) Bright field images of Vero E6 cells infected with SARS-CoV-2 virus. Viral cytopathic effects (CPE) are noted in the infected culture. Scale Bar: 50 µm. (B) IFA images of infected cells (48 hpi) stained for SARS-CoV-2. Mouse monoclonal antibody (MS Ab) targeting Spike and a Guinea pig polyclonal SARS-CoV antibody were used. Mock infected cells were included as negative control. Scale Bar: 25 µm. (C) IFA images show compounds with antiviral activity. Images depict that hydroxychloroquine, interferons, and EIDD-2801 (Molnupiravir) (10µM) are effective in blocking SARS-CoV-2 infection. The mock and infected cells were immunostained with dsRNA antibody, which recognizes double stranded genomic RNA generated during viral replication. 20X magnification. Representative data from three or more independent experiments are presented. Related to Figure 1.

Figure S2

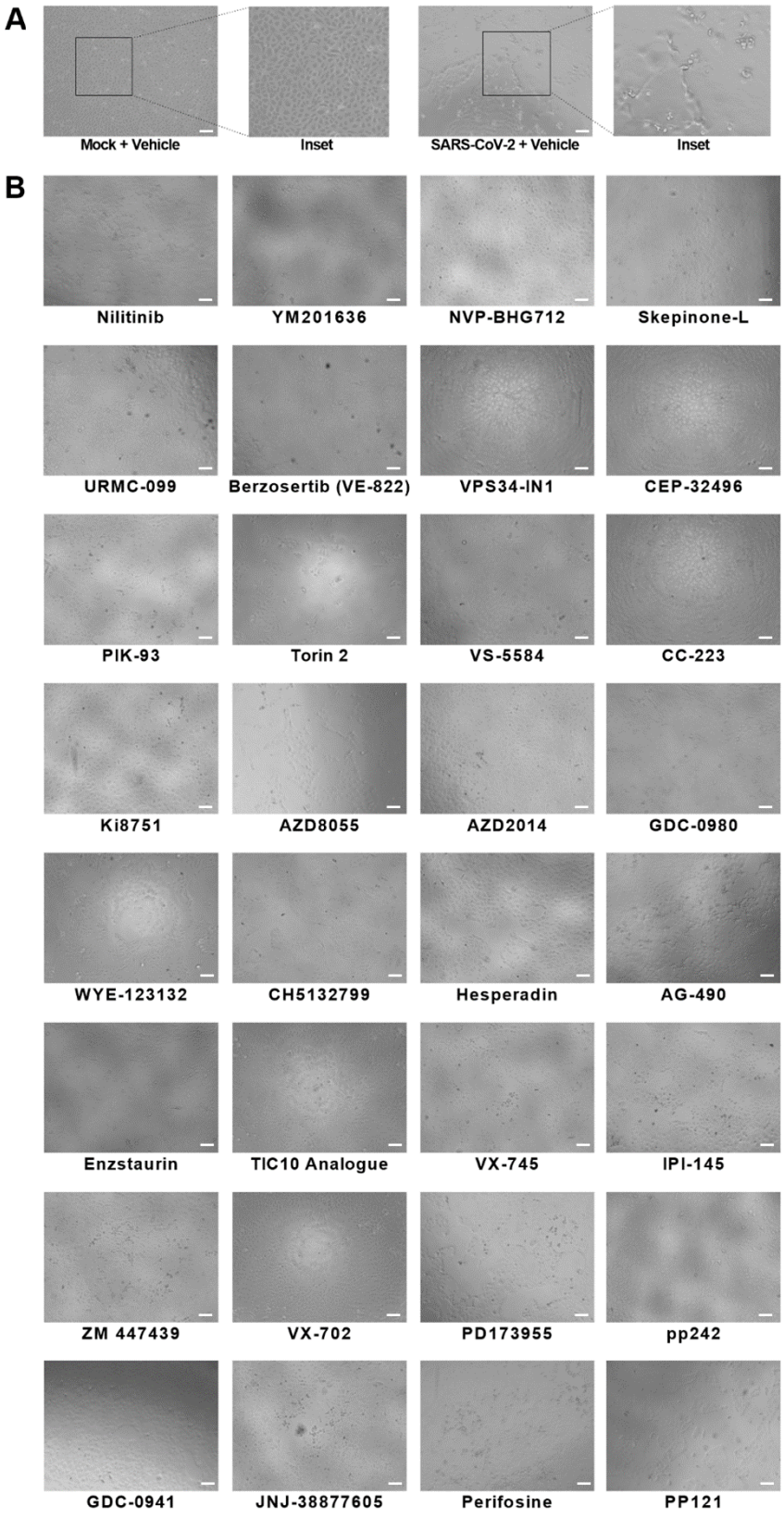
A
Mock + Vehicle
Inset
SARS-CoV-2 + Vehicle
Inset
B
Nilitinib
YM201636
NVP-BHG712
Skepinone-L
URMC-099
Berzosertib (VE-822)
VPS34-IN1
CEP-32496
PIK-93
Torin 2
VS-5584
CC-223
Ki8751
AZD8055
AZD2014
GDC-0980
WYE-123132
CH5132799
Hesperadin
AG-490
Enzstaurin
TIC10 Analogue
VX-745
IPI-145
ZM 447439
VX-702
PD173955
pp242
GDC-0941
JNJ-38877605
Perifosine
PP121

**Figure S2. Primary screen of compounds inhibiting SARS-CoV-2 viral cytopathic effect.** (A) DMSO Vehicle treated Vero E6 cells with SARS-CoV-2 infection had pronounced viral CPE at 48 hpi. Uninfected cells (Mock+vehicle) are included as negative control. Scale Bar: 50 µm. (B) Bright field microscopic images of drug compounds treated SARS-CoV-2 infected cells showing no or reduced level of viral CPE. Scale Bar: 50 µm. Related to Figure 1.

Figure S3

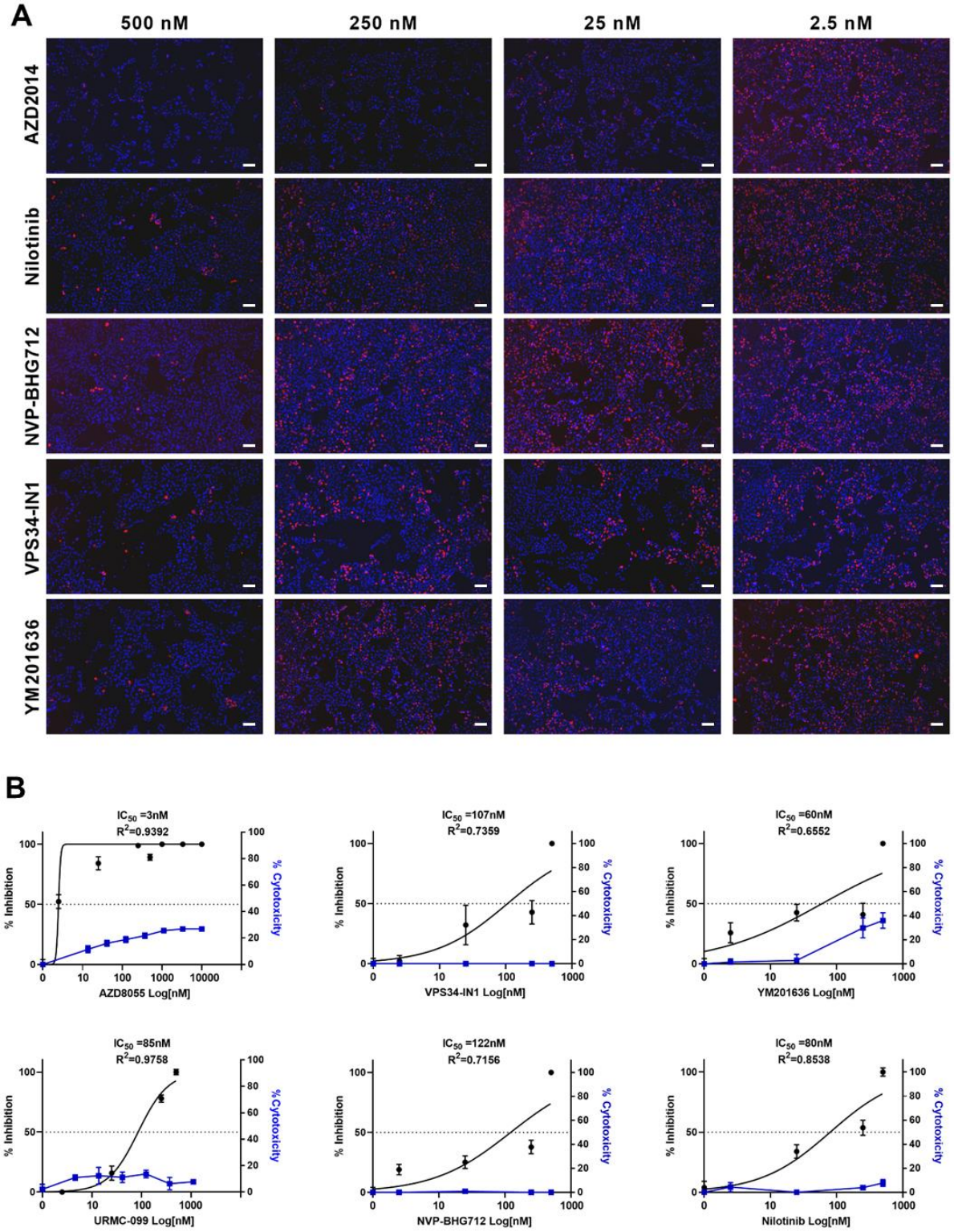
A
500 nM
250 nM
25 nM
2.5 nM
AZD2014
Nilotinib
NVP-BHG712
VPS34-IN1
YM201636
B
IC50 =3nM
R2=0.9392
AZD8055 Log[nM]
IC50 =107nM
R2=0.7359
VPS34-IN1 Log[nM]
IC50 =60nM
R2=0.6552
YM201636 Log[nM]
IC50 =85nM
R2=0.9758
URMC-099 Log[nM]
IC50 =122nM
R2=0.7156
NVP-BHG712 Log[nM]
IC50 =80nM
R2=0.8538
Nilotinib Log[nM]
% Inhibition
% Cytotoxicity

**Figure S3. Secondary Screen in Vero E6 cells.** (A) Immunofluorescent images of SARS-CoV-2 (red) infected Vero E6 cells treated with indicated drug compounds at various concentrations. (B) Graphs show percent inhibition of SARS-CoV-2 infectivity by indicated compounds. Note: IC50 of each compound is shown in the graph. Related to Figure 1.

Figure S4

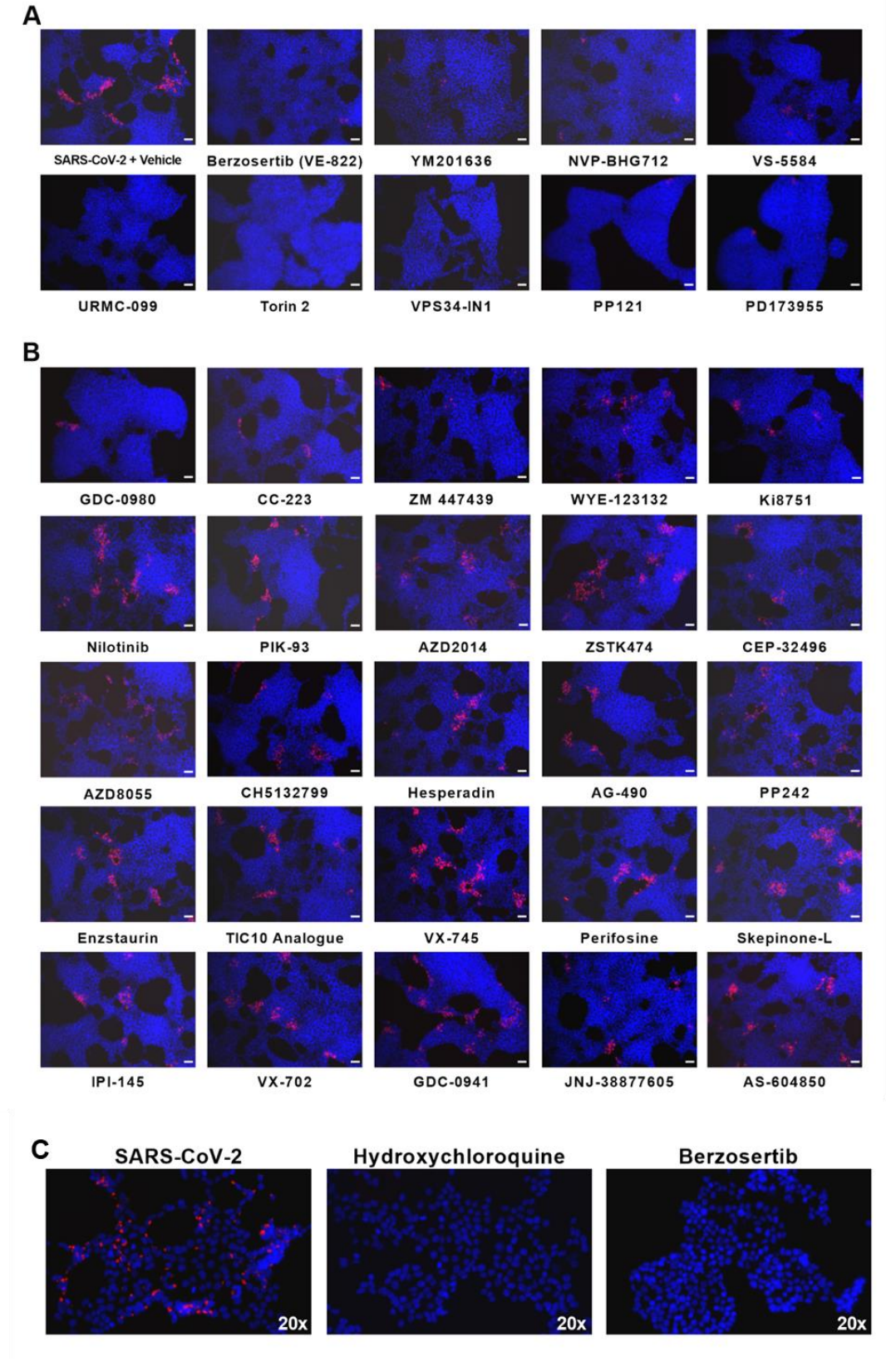
A
SARS-CoV-2 + Vehicle
Berzosertib (VE-822)
YM201636
NVP-BHG712
VS-5584
URMC-099
Torin 2
VPS34-IN1
PP121
PD173955
B
GDC-0980
CC-223
ZM 447439
WYE-123132
Ki8751
Nilotinib
PIK-93
AZD2014
ZSTK474
CEP-32496
AZD8055
CH5132799
Hesperadin
AG-490
PP242
Enzstaurin
TIC10 Analogue
VX-745
Perifosine
Skepinone-L
IPI-145
VX-702
GDC-0941
JNJ-38877605
AS-604850
C
SARS-CoV-2
Hydroxychloroquine
Berzosertib
20x
20x
20x

**Figure S4. Secondary Screen in HEK293-ACE2 cells.** The cells were pre-treated with each of the 34 compounds (250 nM) from the primary screen for 24 hours. The following day the cells were infected with SARS-CoV-2 with an MOI of 0.1. At one day post-infection the cells were fixed in methanol and immunostained to detect SARS-CoV-2 Spike antigen (red). (A) Immunofluorescent images of compounds having potent anti- SARS-CoV-2 activity are shown. Vehicle control with infection was included as reference. (B) Drugs with low or no anti-viral activity at tested dose of 250 nM are presented. Note: Compounds including nilotinib and AZD2014 had not exhibited potent anti-viral activity at tested 250 nM dose level. Scale Bar=25um. (C) IFA images show SARS-CoV-2 (red) infection in untreated cells and hydroxychloroquine (10 μM) treated cells. Complete inhibition of SARS-CoV-2 infection in berzosertib (100nM) treated cells is noted. 20x magnification. Related to Figure 1.

Figure S5

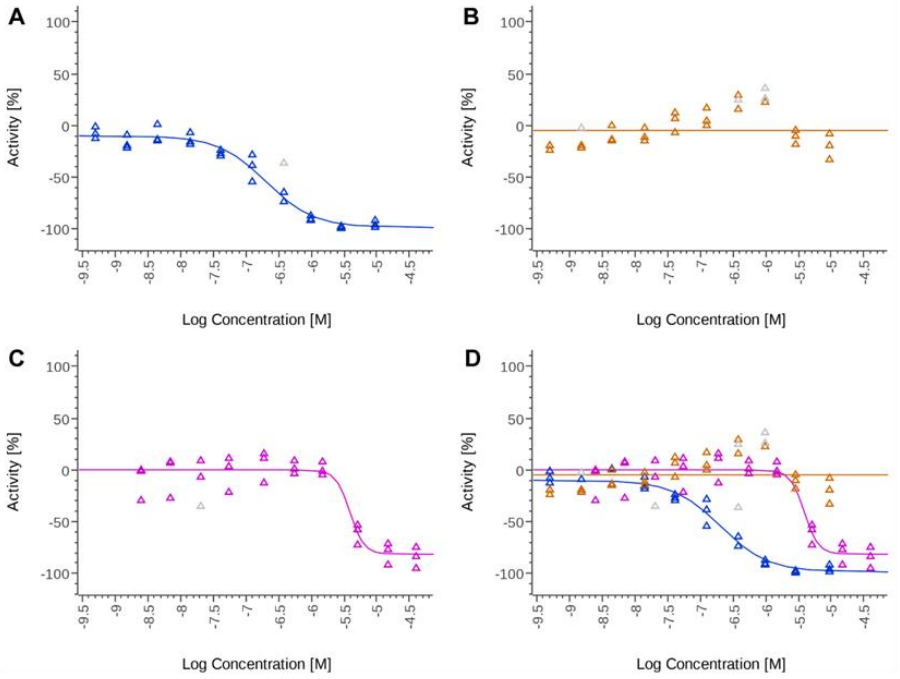
A
B
C
D
Activity [%]
Log Concentration [M]

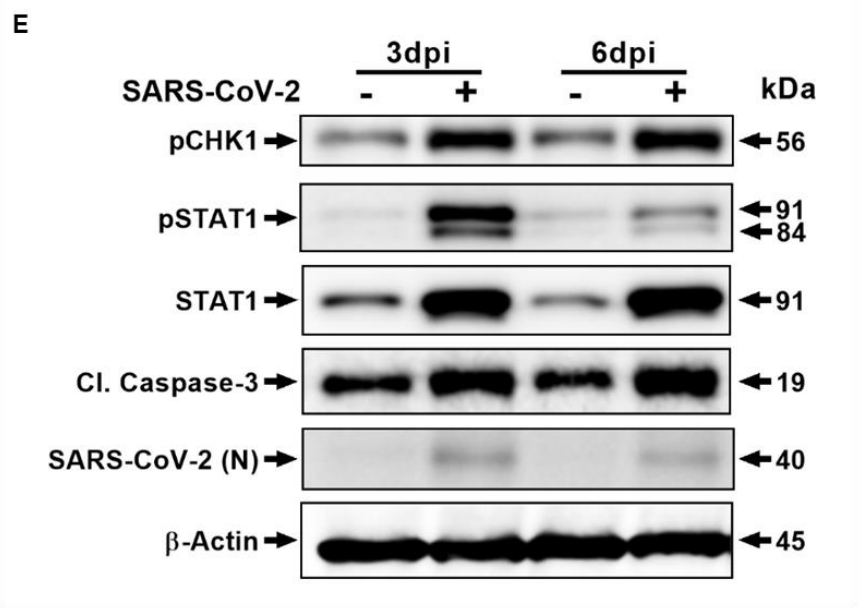
E
3dpi
6dpi
SARS-CoV-2
kDa
pCHK1
pSTAT1
STAT1
Cl. Caspase-3
SARS-CoV-2 (N)
β-Actin
56
91
84
91
19
40
45

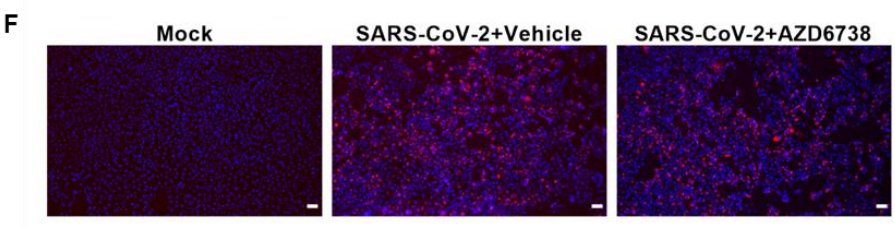
F
Mock
SARS-CoV-2+Vehicle
SARS-CoV-2+AZD6738

**Figure S5. Berzosertib inhibits SARS-CoV-2 replication in human HeLa-ACE2 cells and affects DDR pathway.** (A) Graph shows antiviral activity measured with a SARS-CoV-2 immunofluorescence signal leading to identification of infected cells with 0% activity equals 100% infected cells. (B) total cells per well in SARS-CoV2 infected cell test with 0% activity equaling no change vs. control (C) total cells per well in HeLa-ACE2 uninfected cell control. (D) Overlay of curves in A, B and C. (E) SARS-CoV-2 activates DDR pathway by CHK1 phosphorylation. Western blot analysis shows phosphorylation of key ATR kinase downstream target protein CHK1 in SARS-CoV-2 infected lung proximal airway epithelial cells grown in air-liquid interface (ALI) culture (48hpi). (F) Evaluating additional DNA-Damage Pathway ATR Kinase Inhibitor. Vero E6 cells pre-treated (24 hours) with AZD6738 (10μM) were infected with SARS-CoV-2 48 hours post-infection virus replication was visualized with immunostaining. Scale Bar=100 μm. IFA images show SARS-CoV-2 (red) infection in vehicle or AZD6738 treated cells. No inhibition of SARS-CoV-2 infection in AZD6738 (10μM) treated cells is noted. Related to Figure 3 and 4.

**SUPPLEMENTARY TABLE**

**Table S2.** Drugs compounds selected from primary screen having antiviral activity at 250 nM concentration (Related to Figure 1).

| | **Compound Name** | **Activity** |
|---|---|---|
| 1 | Berzosertib (M6620) | ATR kinase inhibitor |
| 2 | Nilotinib (AMN-107) | Bcr-Abl inhibitor |
| 3 | NVP-BHG712 | EphB4 inhibitor |
| 4 | VPS34-IN1 | Vps34 inhibitor |
| 5 | YM201636 | PIKfyve inhibitor |
| 6 | AZD-2014 (Vistusertib) | Inhibitor mTOR and multiple PI3K isoforms (α/β/γ/δ) |
| 7 | AZD8055 | ATP-competitive mTOR inhibitor |
| 8 | VS-5584 (SB2343) | Dual PI3K/mTOR inhibitor |
| 9 | Torin 2 | Selective mTOR inhibitor |
| 10 | CC-223 (Onatasertib) | mTOR inhibitor |
| 11 | WYE-125132 (WYE-132) | ATP-competitive mTOR inhibitor |
| 12 | PP242 (Torkinib) | mTOR inhibitor |
| 13 | ZSTK474 | Inhibitor of class I PI3K isoforms |
| 14 | GDC-0941 (Pictilisib) | PI3Kα/δ inhibitor |
| 15 | GDC-0980 (RG7422) | Class I PI3K inhibitor for PI3Kα/β/δ/γ |
| 16 | AS-604850 | ATP-competitive PI3Kγ inhibitor |
| 17 | CH5132799 | Inhibitor of class I PI3Ks |
| 18 | IPI-145 (INK1197) | selective PI3K δ/γ inhibitor |
| 19 | PIK-93 | PI3Kγ and PI4KIIIβ inhibitor |
| 20 | Enzastaurin (LY317615) | PKCβ inhibitor |
| 21 | TIC10 Analogue | Inactivates Akt and ERK |
| 22 | Perifosine (KRX-0401) | Akt inhibitor |
| 23 | AG-490 (Tyrphostin B42) | EGFR and JAK2 inhibitor |
| 24 | VX-745 | p38α MAPK inhibitor |
| 25 | Skepinone-L | p38α-MAPK inhibitor |
| 26 | VX-702 | p38α MAPK inhibitor |
| 27 | CEP-32496 | Inhibitor of BRAF(V600E/WT) and c-Raf |
| 28 | ZM 447439 | ATP-competitive inhibitor for Aurora kinases A and B |
| 29 | Hesperadin | Aurora kinase B inhibitor |
| 30 | JNJ-38877605 | ATP-competitive inhibitor of c-Met |
| 31 | Ki8751 | VEGFR2 inhibitor |
| 32 | URMC-099 | Mixed lineage kinase (MLK) inhibitor |
| 33 | PD173955 | Bcr-Abl inhibitor |
| 34 | PP121 | Inhibitor of PDGFR, Hck, mTOR, VEGFR2, Src and Abl |